Sperm-triggered [Ca^{2+}] oscillations and Ca^{2+} homeostasis in the mouse egg have an absolute requirement for mitochondrial ATP production

Rémi Dumollard[1,*], Petros Marangos[1], Greg Fitzharris[1], Karl Swann[2], Michael Duchen[1] and John Carroll[1]

[1]Department of Physiology, University College London, Gower Street, London, WC1E 6BT, UK
[2]Department of Anatomy and Developmental Biology, University College London, Gower Street, London WC1E 6BT, UK
*Author for correspondence (e-mail: r.dumollard@ucl.ac.uk)

Accepted 19 March 2004

Development 131, 3057-3067
Published by The Company of Biologists 2004
doi:10.1242/dev.01181

Summary

At fertilisation, repetitive increases in the intracellular Ca^{2+} concentration, $[Ca^{2+}]_i$, drive the completion of meiosis and initiate the development of the quiescent egg into an embryo. Although the requirement for an ATP supply is evident, the relative roles of potential ATP sources remains unclear in the mammalian egg, and the specific role of mitochondria in $[Ca^{2+}]_i$ regulation as well as in the sperm-triggered [Ca^{2+}] oscillations is unknown.

We have used fluorescence and luminescence imaging to investigate mitochondrial activity in single mouse eggs. Simultaneous imaging of mitochondrial redox state (NADH and flavoprotein autofluorescence) and $[Ca^{2+}]_i$ revealed that sperm-triggered [Ca^{2+}] oscillations are transmitted to the mitochondria where they directly stimulate mitochondrial activity. Inhibition of mitochondrial oxidative phosphorylation caused release of Ca^{2+} from the endoplasmic reticulum because of local ATP depletion. Mitochondrial ATP production is an absolute requirement for maintaining a low resting $[Ca^{2+}]_i$ and for sustaining sperm-triggered [Ca^{2+}] oscillations. Luminescence measurements of intracellular [ATP] from single eggs confirmed that mitochondrial oxidative phosphorylation is the major source of ATP synthesis in the dormant unfertilised egg. These observations show that a high local ATP consumption is balanced by mitochondrial ATP production, and that balance is critically poised. Mitochondrial ATP supply and demand are thus closely coupled in mouse eggs. As mitochondrial ATP generation is essential to sustain the [Ca^{2+}] signals that are crucial to initiate development, mitochondrial integrity is clearly fundamental in sustaining fertility in mammalian eggs.

Key words: Mouse, Egg, Meiosis, Inositol 1,4,5-trisphosphate, Mitochondria, Autofluorescence.

Introduction

In all species that have been studied, fertilisation stimulates an increase in the concentration of cytosolic Ca^{2+} (Stricker, 1999; Dumollard et al., 2002). The increase in [Ca^{2+}] mediates egg activation which comprises cortical granule exocytosis, the resumption of the meiotic cell cycle and recruitment of maternal mRNAs (Kline and Kline, 1992; Swann and Ozil, 1994; Ducibella et al., 2002). In mammals, repetitive Ca^{2+} signals are also thought to be important for pre- and post-implantation development (Jones, 1998; Ozil and Huneau, 2001).

In mice, the fertilisation Ca^{2+} signal takes the form of a series of Ca^{2+} transients that continue for about 4 hours, stopping at pronuclei formation (Marangos et al., 2003). These Ca^{2+} transients are caused by Ins(1,4,5)P_3-induced Ca^{2+} release (IICR) from the endoplasmic reticulum (ER) Ca^{2+} stores. The cytosolic Ca^{2+} is pumped back into the ER by sarco-endoplasmic reticulum Ca^{2+} ATPases (SERCAs) or extruded out of the cell by plasma membrane Ca^{2+} ATPases (PMCAs) (Carroll, 2001; Brini et al., 2003) and Na^+/Ca^{2+} exchangers (Pepperell et al., 1999; Carroll, 2000).

In recent years, mitochondria have been shown to be major regulators of intracellular Ca^{2+} homeostasis (Duchen, 2000; Rizzuto et al., 2000). In cells such as sea urchin (Eisen and Reynolds, 1985) and ascidian eggs (Dumollard et al., 2003), mitochondria sequester Ca^{2+} during the fertilisation Ca^{2+} transients. Ca^{2+} sequestration by mitochondria has two main consequences. First, mitochondria act as passive Ca^{2+} buffers that can regulate intracellular Ca^{2+} release (reviewed by Rizzuto et al., 2000; Duchen, 2000). The second consequence is that Ca^{2+} in the mitochondrial matrix is a 'multisite' activator of oxidative phosphorylation (or mitochondrial ATP synthesis, see Fig. 11): it activates the dehydrogenases of the Kreb's cycle and the electron transport chain (McCormack and Denton, 1993; Hansford, 1994) and has a direct action on the F_0/F_1 ATP synthase (Territo et al., 2000). In somatic cells and in ascidian eggs, mitochondrial Ca^{2+} uptake has been shown to stimulate mitochondrial respiration by promoting the reduction of mitochondrial NAD^+ to NADH (Duchen, 1992; Pralong et al., 1994; Hajnoczky et al., 1995; Dumollard et al., 2003). Furthermore, mitochondrial ATP production may directly regulate intracellular Ca^{2+} release: ATP^{4-} sensitises the Ins(1/4/5)P_3 receptor to activation by Ca^{2+} (Mak et al., 1999; Mak et al., 2001) while Mg^{2+}-complexed ATP is consumed to refill the ER Ca^{2+} stores.

In mammalian oocytes and embryos, mitochondria are the

most prominent organelles, together with the ER and cortical granules (Motta et al., 2000; Sathananthan and Trounson, 2000). Recent studies have revealed that the intrinsic mitochondrial potential of human oocytes programs the developmental fate of embryos through an effect on the ability of oocytes to form a normal meiotic apparatus (Wilding et al., 2003). Furthermore, high-polarised pericortical mitochondria may have a role in the acquisition of oocyte competence and the regulation of early developmental processes (Van Blerkom et al., 2002). Moreover the contribution of mitochondria to Ca^{2+} homeostasis in mammalian eggs is still ill defined. It is known that collapsing mitochondrial electrical potential in mouse eggs impairs Ca^{2+} clearance from the cytosol (Liu et al., 2001) but the precise role mitochondria play in the regulation of sperm-triggered [Ca^{2+}] oscillations remains unclear.

The involvement of mitochondria in maintaining the energetic status of the egg is substantiated by the fact that early development (one- to eight-cell stage) in the mouse is supported by the oxidation of pyruvate and lactate, especially pyruvate (Leese, 1995). Glucose is poorly used because of the block to the regulatory glycolytic enzyme phosphosfructokinase (Barbehenn et al., 1974). Mouse eggs and early embryos can also use glutamine as an energetical substrate that will be oxidised in the mitochondria (Gardner et al., 1989). The mouse egg also possesses sizeable amounts of the enzyme lactate dehydrogenase, which catalyses the oxidation of lactate to pyruvate (Lane and Gardner, 2000). Finally, β-oxidation of intracellular lipids has only been studied in pig embryos, where this pathway does not seem to be used during early development (Sturmey and Leese, 2003). Despite heavy reliance on mitochondria, oxygen consumption of the mouse egg and early embryo is very low compared with oxygen consumption of the blastocyst and mitochondria are thought to be ‘immature’ in the mouse egg and early embryo (Houghton et al., 1996; Trimarchi et al., 2000).

Therefore, in the early mammalian embryo, the source of ATP generation is still a matter of debate. We have investigated the mechanism of coupling ATP supply and demand at fertilisation when demand is increased. Furthermore, we use mitochondrial inhibitors to investigate the importance of mitochondrial function in providing for ATP demand generated by the mechanisms of Ca^{2+} homeostasis and by sperm-triggered Ca^{2+} oscillations.

Materials and methods

Oocytes

Mature (MII) oocytes were recovered from 21- to 24-day-old MF1 mice previously administered 7 U of pregnant mares serum gonadotrophin (PMSG) and 5 U human Chorionic Gonadotrophin (hCG) at a 48-hour interval. Mice were culled by cervical dislocation and the oviducts removed 14-16 hours post-hCG. Cumulus masses were released into HEPES-buffered KSOM (H-KSOM) (Biggers et al., 2000) containing 1 mg/ml BSA by rupture of the oviduct with a 27 gauge needle. When it was necessary to remove the cumulus cells, hyaluronidase (150 U ml^{-1}) was added to the H-KSOM. Cumulus-free oocytes were collected and washed in H-KSOM three times and placed in a drop of the same medium under mineral oil.

In vitro fertilisation

For in vitro fertilisation, epididymis were dissected from proven fertile MF1 males that had been culled by cervical dislocation. The epididymis were transferred into 1 ml drops of pre-equilibrated (5% CO_2 in air) T6 medium containing 10 mg ml^{-1} bovine serum albumin (BSA, Fraction V Sigma). Sperm were released by puncturing the epididymis with a 27 gauge needle. The sperm were placed in the incubator for 20 minutes during which time they dispersed into a suspension. This suspension was diluted 1:5 in drops of the same medium under oil and incubated for another 2-3 hours for capacitation to occur. IVF was performed in drops of H-KSOM under paraffin oil. The zona pellucida of MII stage oocytes were removed by a brief exposure to acidified Tyrode’s solution (Sigma). Sperm were added to the zona-free MII oocytes at a 1:10 dilution of the capacitated sperm suspension. For imaging experiments, zona-free oocytes were placed in a heated chamber with a cover glass base containing 0.5 ml of H-KSOM without BSA for 3-5 minutes. 0.5 ml of complete H-KSOM was then added to the chamber and the media was covered with oil to prevent evaporation. Capacitated sperm were then added to the chamber at time t=0 except where mentioned.

Microinjection

Cells were pressure injected with a micropipette and Narishige manipulators mounted on an inverted Leica microscope essentially as described previously (FitzHarris et al., 2003). Oocytes were placed in a drop of H-KSOM covered with mineral oil and immobilised with a holding pipette. To penetrate the plasma membrane, a brief over-compensation of negative capacitance was applied.

Measurement of intracellular Ca^{2+} and photolysis of caged Ins(1,4,5)P_3

Intracellular Ca^{2+} was measured using Fura red, Fura 2, Indo 1 or Rhod2 (Molecular Probes). Oocytes were loaded in H-KSOM containing 2 μM of the acetoxymethyl ester (AM) form of the Ca^{2+} dyes and 0.02% pluronics for 10 minutes at 37°C. After loading, oocytes were placed in a drop of H-KSOM under oil in a chamber with a coverslip. The chamber was placed in a heated stage on a Zeiss axiovert microscope or on a Zeiss LSM 510 confocal microscope. Excitation light (Fura red, 490 nm; Indo 1, 365 nm; Fura 2, 340 and 380 nm; Rhod 2, 543 nm) was delivered by a monochromator, while emission was collected using a filter (Fura red, 600 nm longpass; Rhod 2, 580 nm longpass; Indo 1, 390-430 nm and 435-480 nm bandpass; Fura 2, 520 nm longpass) placed in front of a cooled CCD camera (MicroMax, Princeton Instruments). Measurements where obtained by averaging the signal collected in a region of interest (ROI) drawn in the centre of the egg (see Figs 1 and 3 for typical examples of such ROIs).

Caged Ins(1,4,5)P_3 was microinjected as described above to an estimated final concentration of 50 μM. Photo-release was performed 30-60 minutes after microinjection by brief timed exposures of injected oocytes to UV light (360 nm). For uncaging experiments, $[Ca^{2+}]_i$ was measured using Rhod2 AM to allow the simultaneous measurement of FAD^{++} in the green channel and $[Ca^{2+}]_i$ in the red channel. Rhod2 AM partitions into the cytosol and in some peripheral vesicles of mouse oocytes (see Fig. 3B) and not into mitochondria as it has been published elsewhere (Liu et al., 2001) or as it occurs in somatic cells (Duchen, 2000).

The excitation wavelengths and camera exposure times were controlled using Metafluor software (epifluorescence microscope) or the LSM 510 software (confocal microscope).

Autofluorescence measurements

NADH fluorescence was excited with UV light (360 nm or the 364 nm line of the UV laser of the confocal microscope) and emission was collected using a 470 nm longpass or a 435-485 bandpass filter. Oxidised flavoproteins (FAD^{++}) fluorescence was excited with the 458 nm line of an argon laser or with a 440-490 nm bandpass filter while emitted fluorescence was collected through either a 520 nm longpass filter or a 505-550 nm bandpass filter. Measurements were obtained by averaging the signal collected in a region of interest (ROI) drawn

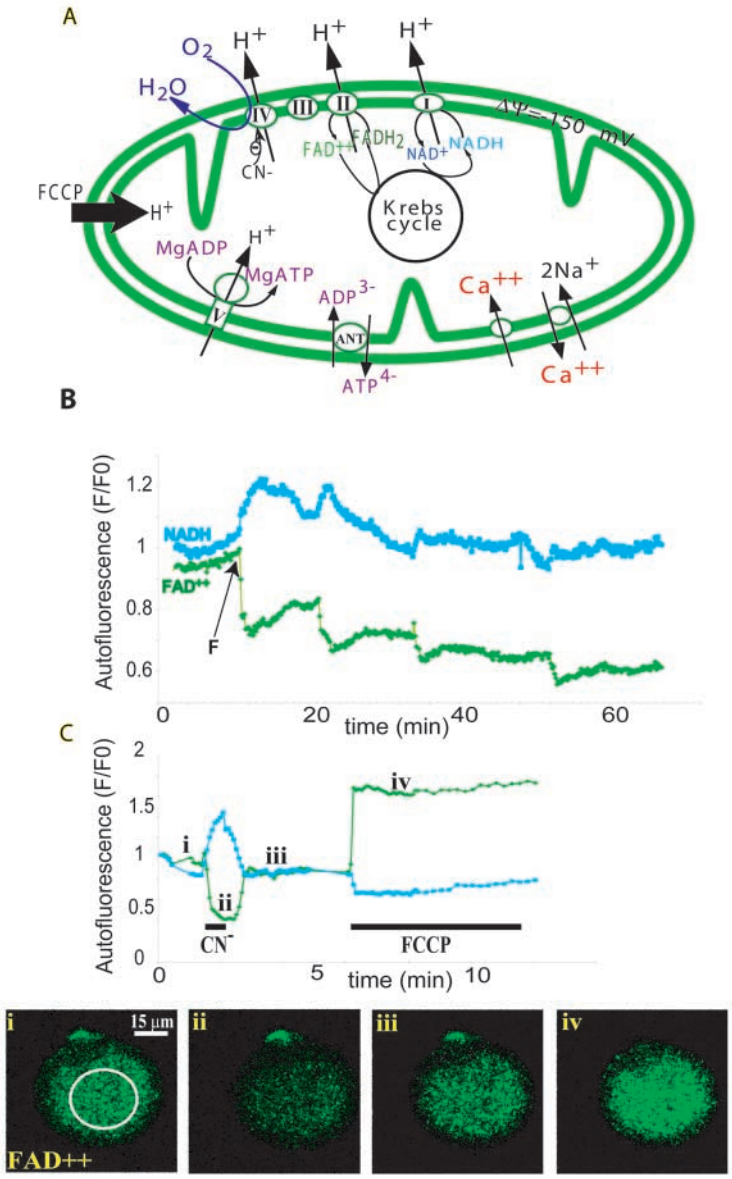

Fig. 1. Synchronous oscillations of NADH and FAD^{++} autofluorescence at fertilisation. (A) Ca^{2+} fluxes and oxidative phosphorylation in the mitochondria. The supply of substrate (such as pyruvate) to the Kreb's cycle promotes the reduction of NAD^{+} to NADH and of FAD^{++} to $FADH_2$. NADH is then oxidised by complex I in the respiratory chain, whereas $FADH_2$ is oxidised at complex II. The electrons are then transferred to complexes III and IV to reduce O_2 to H_2O. In the process, protons are translocated across the inner mitochondrial membrane, generating a potential gradient of approximately –150 mV ($\Delta\Psi$). ATP synthesis takes place at complex V or F0/F1 synthase, the inward flux of protons through the synthase provides the energy necessary to phosphorylate ADP. ATP is then transported out of the mitochondria by the adenine nucleotide translocase (ANT). Ca^{2+} enters the mitochondria through the Ca^{2+} uniporter, while it is extruded via the action of a Na^{+}/Ca^{2+} exchanger. The actions of CN^{-} and FCCP are also indicated. (B) Variations in NADH (blue trace) and FAD^{++} (green trace) observed at fertilisation of a mouse egg (n=6). Time 0 corresponds to the time of insemination. F indicates the time of fertilisation. (C) Changes in NADH (blue trace) and FAD^{++} (green trace) autofluorescence measured inside the ROI shown in (i), upon perfusion of 2 mM CN^{-} (provoking full reduction of NADH and FAD^{++}) and of 1 µM FCCP (provoking full oxidation of NADH and FAD^{++}). (i-iv) Images of FAD^{++} autofluorescence of a mouse egg at times indicated on the graph.

in the centre of the egg (see Figs 1 and 3 for typical examples of such ROIs). The measurements displayed (F/F0) in the graph are normalised values with regard to the first value of the experiment (F0).

Monitoring of mitochondrial potential

Eggs were incubated for 15 minutes in H-KSOM containing 10 µg/ml of the lipophilic cationic dye Rhod 123 (exc: 488 nm, em: 520 nm). With this loading protocol, internalisation of the dye in the mitochondria quenches the Rhod123 fluorescence and depolarisation can be seen as an increase in green fluorescence, while a hyperpolarisation is seen as a decrease in Rhod 123 fluorescence (for details, see Duchen and Biscoe, 1992). For imaging of the mitochondria, eggs were incubated for 15 minutes in H-KSOM containing 1 µg/ml of Mitotracker Green (Molecular Probes, Netherlands) or 100 nM of tetramethylrhodamine methyl ester (TMRM, Molecular Probes) and then imaged on the confocal microscope. Measurements were obtained by averaging the signal collected in a region of interest (ROI) drawn in the centre of the egg (see Figs 1 and 3 for typical examples of such ROIs).

Labelling of endoplasmic reticulum

To label the endoplasmic reticulum, DiI_{18} (Molecular Probes) was microinjected as a saturated solution in soybean oil (Sigma) 30 minutes before imaging. Imaging was performed using a Zeiss LSM 510 microscope. DiI_{18} was excited using the 514 nm line of an Argon laser and the emitted light collected using a 600 nm longpass filter.

Measurement of intracellular ATP in a single egg

The luminescent ATP indicator firefly luciferase (Calbiochem) (Allue et al., 1996; Jouaville et al., 1999) was injected into unfertilised mouse eggs as described above. The concentration of recombinant luciferase protein in the injection pipette was 2 mg ml^{-1}. The eggs were then incubated in H-KSOM containing 100 µM luciferin for 30 minutes before any measurements could be made. The luminescence emanating from individual luciferase-injected eggs was monitored with an imaging photon detector (Photek, UK, using software and a system design provided by science wares, www.sciencewares.com).

Perfusion of substrates and inhibitors

The mitochondrial uncoupler FCCP (1 µM, Sigma) as well as inhibitors of the respiratory chain [complex I, rotenone (5 µM, Sigma); complex II, malonate (20 mM, Sigma); complex IV, CN^{-} (1 mM, Merck); complex V, F0/F1 synthase oligomycin (60 µM, Sigma)] were added to the chamber as 10× solutions. The energetical substrate pyruvate (2 mM, Sigma) was also added as 10× solution. Thapsigargin (Calbiochem) was used at 20 µM final concentration.

Results

Autofluorescence oscillations during sperm-triggered [Ca^{2+}] oscillations

In somatic cells, cytosolic Ca^{2+} transients can stimulate the Kreb's cycle and hence mitochondrial oxidative phosphorylation (McCormack and Denton, 1993; Duchen,

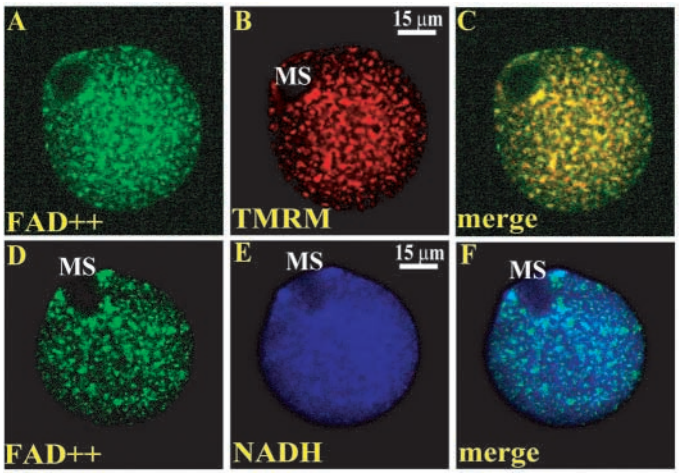

Fig. 2. Imaging of mitochondrial autofluorescence. (A-C) Simultaneous imaging of FAD^{++} autofluorescence (green, A) and mitochondria using the potentiometric dye TMRM (red, B). Merging the image of mitochondria and of autofluorescence (C) clearly shows that the FAD^{++} autofluorescence colocalises with mitochondria. (D-F) Simultaneous imaging of FAD^{++} (D, green) and NADH (E, blue). Merging the NADH and FAD^{++} images (F) shows that a significant part of the NADH signal is cytosolic. MS, meiotic spindle.

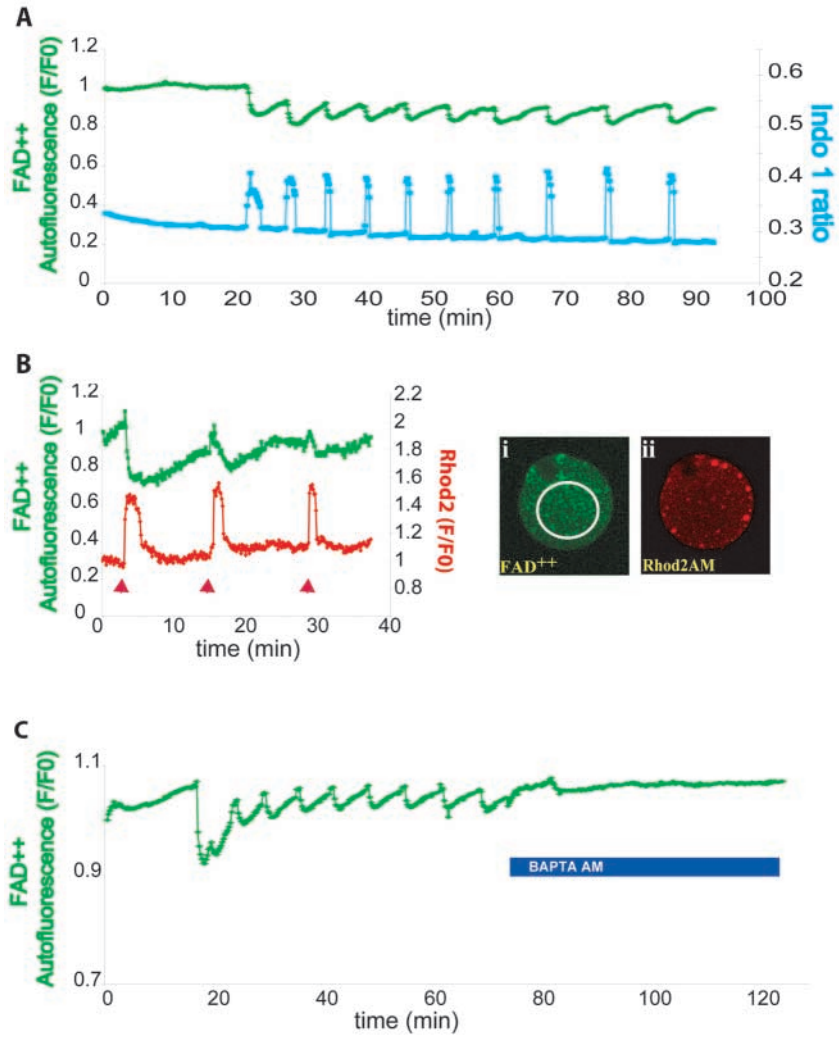

1992). In order to explore the impact of Ca^{2+} signals on mitochondrial function, we used changes in mitochondrial autofluorescence to monitor changes in redox state at fertilisation in mouse eggs.

Redox fluorometry based on intrinsic fluorescence of reduced pyridine nucleotides (NADH and NADPH) and oxidised flavoproteins has been a useful tool for studying cellular energy metabolism (reviewed by Master and Chance, 1993; Duchen 2000; Duchen et al., 2003). We imaged NADH, a reducing equivalent formed by the Kreb's cycle that is oxidised to NAD^+ at complex I of the mitochondrial electron transport chain (Fig. 1A), and flavoproteins, which form an integral component of complex II of the electron transport chain (Fig. 1A). Prior to addition of sperm (at time t=0) the NADH and FAD^{++} autofluorescence was constant. Within 10 minutes of addition of sperm, synchronous oscillations in [NADH] and [FAD^{++}] could be observed (Fig. 1B; n=6). These oscillations correspond to reduction of NAD^+ and FAD^{++} as increases in NADH fluorescence are mirrored by decreases in FAD^{++} fluorescence.

The redox state is readily manipulated by pharmacological inhibition or stimulation of the respiratory chain. Inhibition of respiration by the inhibitor of complex IV CN^- causes maximal reduction of NAD^+ and FAD^{++}, seen as an increase in NADH fluorescence and a decrease in FAD^{++} fluorescence (Fig. 1C, part i), while the mitochondrial uncoupler FCCP causes maximal oxidation of NADH and FAD^{++}, seen as a decrease in NADH fluorescence and an increase in FAD^{++} fluorescence (Fig. 1C, part iv).

The distribution of FAD^{++} autofluorescence on confocal microscopy colocalised with the distribution of the potentiometric dye, TMRM (Fig. 2A-C), which selectively stains energised mitochondria (see Duchen et al., 2003), confirming the mitochondrial origin of the FAD^{++} signal. When imaged simultaneously from a single egg, NADH and FAD^{++} also had a similar mitochondrial distribution (Fig. 2D,E),

Fig. 3. Oscillations in FAD^{++} autofluorescence are stimulated by fertilisation induced Ca^{2+} transients. (A) Variations in $[Ca^{2+}]_c$ (measured with indo 1 AM, blue trace) and FAD^{++} autofluorescence (green trace) observed at fertilisation of a mouse egg (n=20). Time 0 corresponds to the time of insemination. (B) Variations in $[Ca^{2+}]_i$ (measured with rhod 2 AM, red trace) and FAD^{++} autofluorescence (green trace) in a mature mouse egg injected with caged Ins(1,4,5)P_3 (n=10). A UV flash (red arrowhead) releases Ins(1,4,5)P_3 in the egg and triggers a Ca^{2+} transient accompanied by a transient decrease in FAD^{++} autofluorescence. i and ii show the same egg as in Fig. 2D-F with the FAD^{++} signal (i) and Rhod2 AM (ii) signal that have markedly different distributions. This suggests that, under our conditions, rhod2 AM does not partition into mitochondria of the mouse egg. The ROI (white circle in i) used to obtain the measurements is drawn. (C) Oscillations of FAD^{++} autofluorescence are stopped by the addition of 5 μM BAPTA AM to the chamber (the presence of BAPTA AM is indicated by a bar under the graph, n=8)

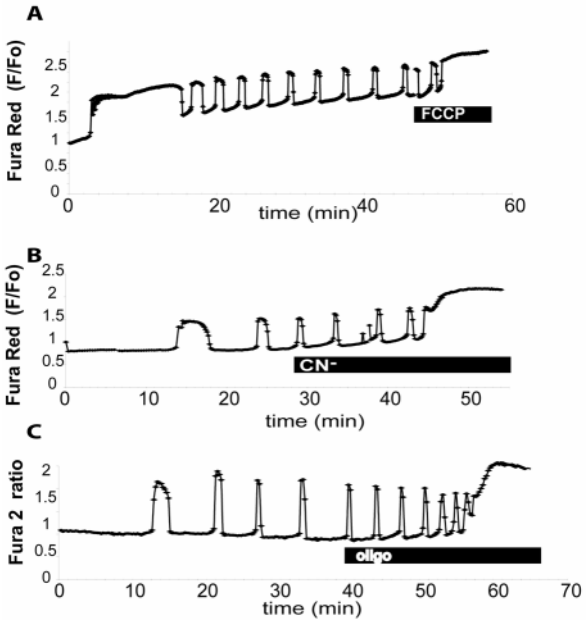

Fig. 4. Inhibition of sperm-triggered $[Ca^{2+}]$ oscillations by mitochondrial inhibitors. Variations of $[Ca^{2+}]_i$ observed at fertilisation (measured with fura red AM in A and B or with fura 2 AM in C). 1 μM FCCP (A), 2 mM CN^- (B) or 60 μM oligomycin (C) are added to the chamber as indicated by the bar under the graph.

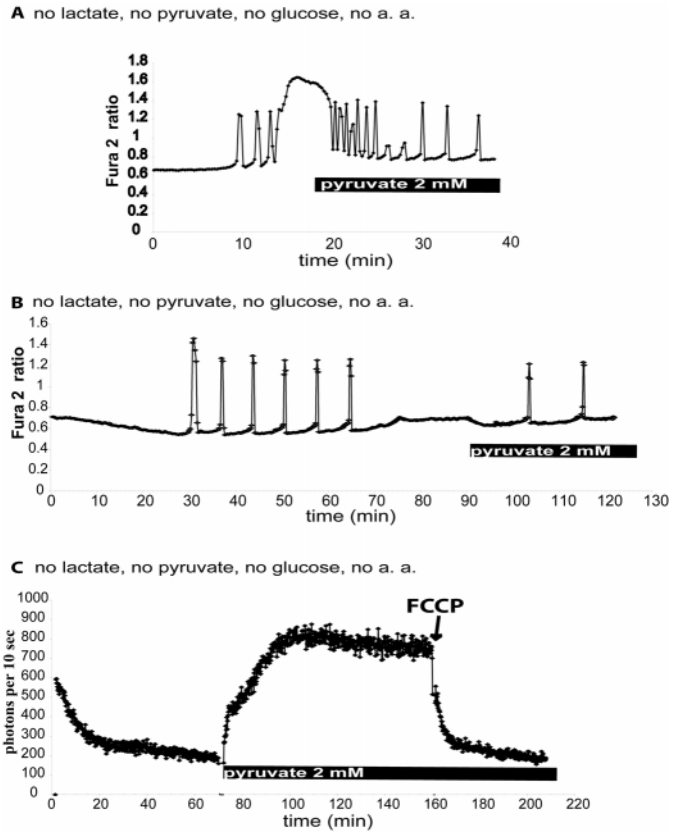

Fig. 5. Effect of energetic substrates starvation on sperm-triggered $[Ca^{2+}]$ oscillations and cellular [ATP]. (A,B) Mature eggs are incubated in M2 medium without lactate, pyruvate, glucose and amino acids for 2 hours and then fertilised. Where indicated, 2 mM pyruvate is added to the dish. The lack of energetic substrates disrupts the sperm-triggered $[Ca^{2+}]$ oscillations with either $[Ca^{2+}]_i$ remaining high after a Ca^{2+} transient (A, n=12) or with $[Ca^{2+}]_i$ remaining low (B, n=11). (C) Changes in $[ATP]_i$ upon withdrawal of energetic substrates (n=7). An egg was placed in M2 medium without energetic substrates for 30 minutes before the start of the recording, then, where indicated, 2 mM pyruvate or 1 μM FCCP was added.

although the NADH image showed relatively high fluorescence in the cytosol, indicating that a significant component of the NADH signal is cytosolic. By contrast, the FAD^{++} signal was more clearly restricted to mitochondria (Fig. 2A-D).

In order to explore the relationship between FAD^{++} oscillations and $[Ca^{2+}]_i$, the two signals were measured simultaneously using indo 1 to monitor $[Ca^{2+}]_i$ while monitoring FAD^{++} autofluorescence. Upon fertilisation, oscillations of $[FAD^{++}]$ were seen concomitant with $[Ca^{2+}]$ oscillations (Fig. 3A). Each $[Ca^{2+}]$ transient was associated with a decrease in FAD^{++} autofluorescence that recovered slowly. The Ca^{2+} dependence of these oscillations of FAD^{++} autofluorescence was confirmed, as triggering a $[Ca^{2+}]$ transient by uncaging Ins(1,4,5)P_3 in the egg also elicited a transient decrease in FAD^{++} autofluorescence (Fig. 3B). The requirement for $[Ca^{2+}]$ oscillations was demonstrated by adding 5 μM BAPTA AM to fertilised eggs (Fig. 3C, n=8). This amount of BAPTA AM is able to stop the $[Ca^{2+}]$ oscillations (Lawrence et al., 1998) (Fig. 3C shows that BAPTA AM stopped the oscillations in autofluorescence).

Together, these results show that sperm-triggered $[Ca^{2+}]$ oscillations stimulate mitochondrial oxidative phosphorylation in the mouse egg, suggesting that the Ca^{2+} signal is transmitted directly to the mitochondrial matrix and that it serves to upregulate mitochondrial oxidative phosphorylation.

Mitochondrial ATP production is necessary to sustain sperm-triggered $[Ca^{2+}]$ oscillations

In order to characterise the role played by mitochondria in the regulation of sperm-triggered $[Ca^{2+}]$ oscillations, we perfused mitochondrial inhibitors onto fertilised eggs. FCCP, a protonophore that collapses the mitochondrial potential, disrupted the $[Ca^{2+}]$ oscillations after a couple of minutes (n=5, Fig. 4A). Ca^{2+} homeostasis was disrupted and the $[Ca^{2+}]_c$ failed to recover after a Ca^{2+} transient. CN^-, an inhibitor of complex IV of the mitochondrial respiratory chain also disrupted $[Ca^{2+}]$ oscillations (n=5, Fig. 4B). Oligomycin, which inhibits mitochondrial ATP synthesis without depolarising the mitochondria (see Fig. 8C) had a very similar effect on the $[Ca^{2+}]$ oscillations (n=7, Fig. 4C). After adding oligomycin, the frequency of the $[Ca^{2+}]$ oscillations first increased and then the $[Ca^{2+}]_c$ failed to recover after a $[Ca^{2+}]$ transient.

Finally, mouse eggs were starved of mitochondrial substrates by incubation in a medium without lactate, pyruvate, glucose and amino acids for 2-4 hours before fertilisation (Fig. 5). In this situation, the egg can be fertilised but the $[Ca^{2+}]$ oscillations were inhibited with either a premature arrest of $[Ca^{2+}]$ oscillations (Fig. 5B, n=11) or the $[Ca^{2+}]_c$ failed to recover after a Ca^{2+} transient (Fig. 5A, n=12). Upon addition of 2 mM pyruvate, the $[Ca^{2+}]_c$ recovered and the $[Ca^{2+}]$

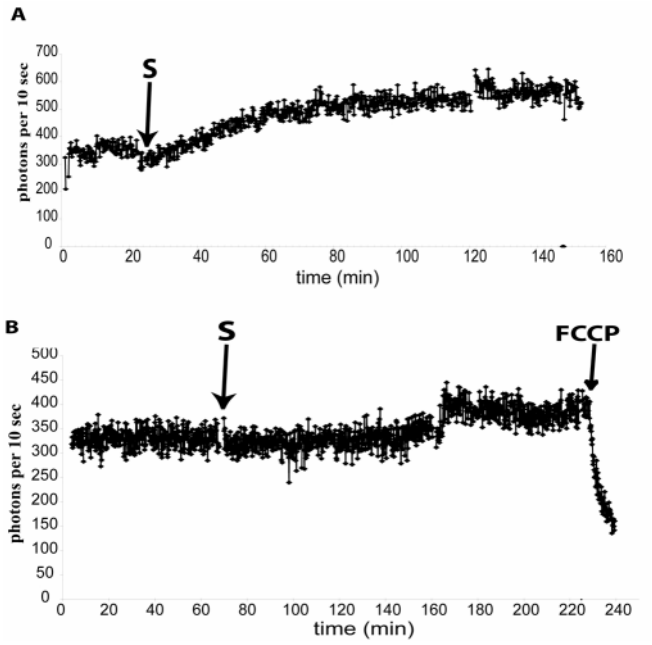

Fig. 6. Fertilisation does not cause a decrease in ATP levels in single eggs. (A,B) Measurements of bulk cytosolic [ATP] in fertilised eggs (A, *n*=9; B, *n*=16). Luminescence recording of an egg injected with firefly luciferase. Sperm (S) was added when indicated by the arrow and, in B, FCCP was added when indicated by the second arrow. The time of fertilisation is ~15-30 minutes after sperm addition. Fertilisation was confirmed by the presence of the second polar body 90 minutes after sperm addition.

oscillations subsequently resumed (*n*=7, Fig. 5A,B). Measuring the $[ATP]_c$ during such experiments showed that the omission of energetic substrates entrains a decrease in $[ATP]_c$ that completely recovers upon pyruvate addition (*n*=7, Fig. 5C). Together, these results demonstrate that mitochondrial oxidative phosphorylation is necessary to sustain the sperm-triggered $[Ca^{2+}]$ oscillations.

Fertilisation is associated with an increased ATP demand coupled with cortical granules exocytosis, chromosome disjunction, polar body extrusion and, as shown above, Ca^{2+} homeostasis. In order to assess the use of ATP at fertilisation, we measured the variations of bulk cytosolic [ATP] by measuring the luminescent signal emitted by injected firefly luciferase (Allue et al., 1996) in fertilised eggs. Fig. 6A,B show two examples of such experiments: in nine out of 25 fertilised eggs $[ATP]_i$ is seen to undergo a gradual increase (Fig. 6A), whereas in 16 out of 25 fertilised eggs there was no significant increase in $[ATP]_i$ in the course of the experiment (Fig. 6B). This finding suggests that the energy demand at fertilisation is matched by energy supplies, and indicates that ATP synthesis is stimulated at fertilisation to a level that allows the maintenance of intracellular ATP levels.

Mitochondrial oxidative phosphorylation is necessary to maintain the resting $[Ca^{2+}]_c$

Mitochondrial activity is clearly essential for sustaining $[Ca^{2+}]$ oscillations in response to sperm. We next explored the role of mitochondria in defining $[Ca^{2+}]_i$ levels in resting, non stimulated oocytes. Mature metaphase II-arrested mouse oocytes maintain a steady resting $[Ca^{2+}]_c$ before fertilisation. Perfusions of FCCP (1 μM) or of CN^- (2 mM) induced a rapid increase of $[Ca^{2+}]_i$ (Fig. 7A, *n*=15; Fig. 7C, *n*=20). This Ca^{2+} increase was biphasic, consisting of an initial increase of low amplitude followed after several minutes by a secondary increase of large amplitude until a new steady state level is attained. The first $[Ca^{2+}]$ increase induced by the mitochondrial inhibitors was

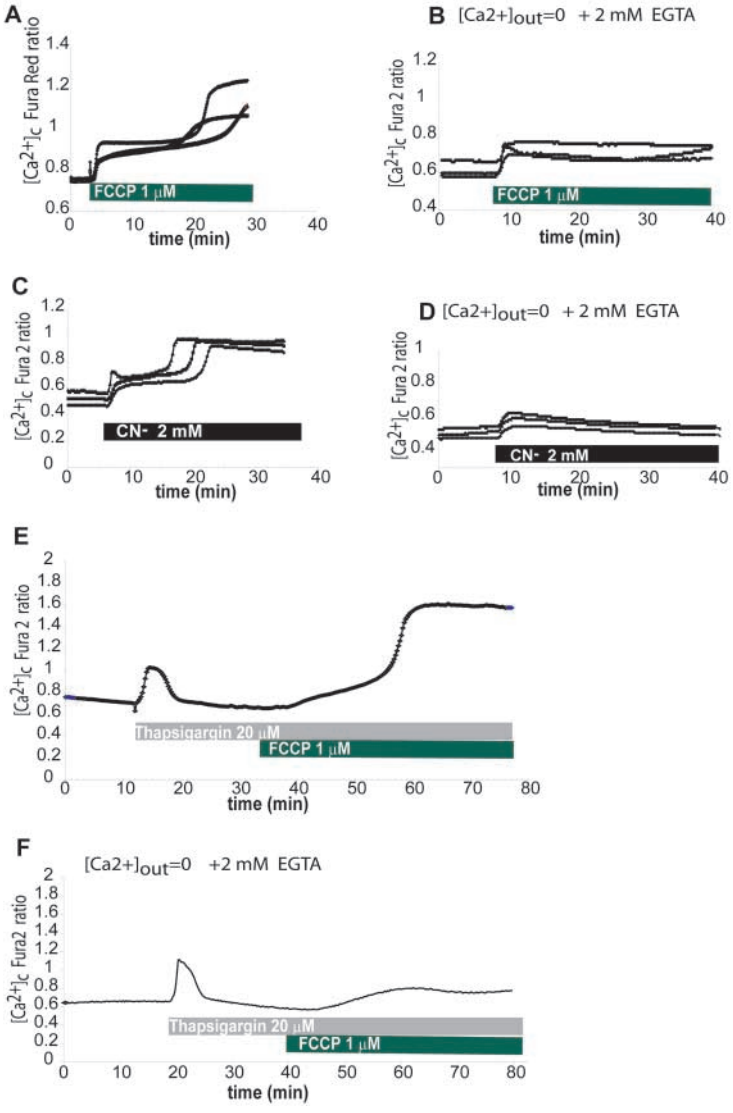

Fig. 7. Mitochondrial inhibitors cause an increase in resting $[Ca^{2+}]_i$ in mature eggs. (A,B) Increase in $[Ca^{2+}]_i$ induced by addition to an unfertilised egg of FCCP (1 μM) in normal H-KSOM medium (A) or in H-KSOM without Ca^{2+} and supplemented with 2 mM EGTA (B). (C,D) Increase in $[Ca^{2+}]_i$ induced by addition to an unfertilised egg of CN^- (2 mM) in normal H-KSOM medium (C) or in H-KSOM without Ca^{2+} and supplemented with 2 mM EGTA (D). (E,F) Variations of $[Ca^{2+}]_i$ induced by sequential addition to an unfertilised egg of 20 μM thapsigargin and FCCP (1 μM) in normal H-KSOM (E) or in H-KSOM without Ca^{2+} (F).

observed even in the absence of external Ca^{2+}, indicating that it was not due to Ca^{2+} influx from the extracellular medium (Fig. 7B, *n*=15; Fig. 7D, *n*=10). Moreover emptying the ER Ca^{2+} stores with thapsigargin before perfusing FCCP prevented the rapid early Ca^{2+} increase (Fig. 7E, *n*=12), suggesting that the source of Ca^{2+} for this $[Ca^{2+}]$ increase resides in the ER stores and does not represent release of mitochondrial Ca^{2+}. In a normal medium containing Ca^{2+}, the secondary Ca^{2+} increase was still observed after emptying the ER stores (Fig. 7E), but it was completely inhibited by clamping external Ca^{2+} to zero with 2 mM EGTA (Fig. 7F, *n*=8), suggesting that the secondary increase represents Ca^{2+} influx.

The $[Ca^{2+}]$ increase induced by mitochondrial inhibitors is due to ATP depletion

Application of FCCP and CN^- depolarise the mitochondria, thus inhibiting Ca^{2+} sequestration by mitochondria. It also impairs mitochondrial ATP production leading to a decrease in $[ATP]_i$ that is dependent on the rate of ATP consumption. The $[Ca^{2+}]$ increase induced by mitochondrial inhibitors may be due to the inhibition of Ca^{2+} uptake by mitochondria or, alternatively, to ATP depletion in the egg. In order to discriminate between these two possibilities, mitochondrial ATP synthesis was blocked with oligomycin an inhibitor of the F_0/F_1 ATP synthase (Fig. 8C). Perfusion of oligomycin caused a similar biphasic increase in $[Ca^{2+}]$ (Fig. 8A, *n*=25) without provoking mitochondrial depolarisation (see next section). This observation strongly implies that the Ca^{2+} leak from the ER and the secondary Ca^{2+} increase caused by Ca^{2+} influx across the plasma membrane are due to ATP depletion in the egg and not to impaired mitochondrial Ca^{2+} sequestration.

Perfusion with either oligomycin (Fig. 8B, *n*=13) or FCCP (Fig. 5C, Fig. 6B) caused a decrease in $[ATP]_i$. That oligomycin alone should cause a rapid loss of $[ATP]_i$ strongly suggests: (1) that mitochondrial oxidative phosphorylation provides the major mechanism to sustain ATP in the resting mature MII oocyte and (2) that there must be a high consumption of ATP in these oocytes to cause a rapid fall after synthesis is stopped.

Mitochondrial membrane potential and activity of the ATP synthase in mouse eggs

The mitochondrial potential is established by the translocation of protons from the mitochondrial matrix to the intermembrane space via the activity of the complexes I, III and IV of the respiratory chain residing in the inner mitochondrial membrane. This gradient is to some extent dissipated by proton influx through the ATP synthase (Fig. 1A) in the process of ATP generation.

By measuring mitochondrial potential with Rhod123 using a dequench protocol (see Materials and methods), we found that oligomycin caused hyperpolarisation of the mitochondrial potential concomitant with the early $[Ca^{2+}]$ increase (Fig. 8A, *n*=25; Fig. 9B, *n*=4). This observation demonstrates that the mitochondrial ATP synthase is active in the mature MII egg and that oligomycin application blocked a resting proton flux into the mitochondrial matrix (see Fig. 8C).

The role of mitochondrial oxidative phosphorylation in maintaining resting $[Ca^{2+}]$ was further examined using a range of respiratory chain inhibitors. The sequential inhibition of complexes I, II and IV by rotenone, malonate and

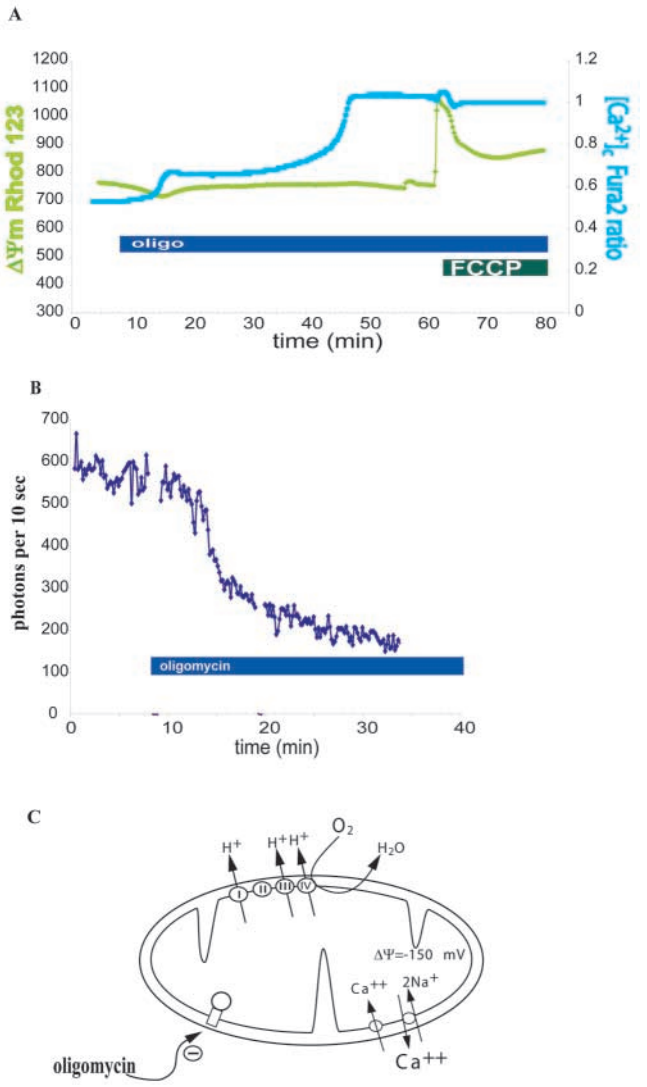

Fig. 8. Mitochondrial inhibitors cause an increase in resting $[Ca^{2+}]_c$ by depleting ATP levels in mature eggs. (A) Simultaneous measurement of $[Ca^{2+}]_i$ (using fura 2 AM) and of ΔΨm [using Rhod 123 (compare with Materials and methods)] in mature eggs. Where indicated, oligomycin (60 μM) and FCCP (1 μM) are added to the bath. (B) Photon emission of a single egg injected with luciferase. Where indicated, oligomycin (60 μM) and FCCP (1 μM) are added to the bath. The background luminescence count was of six photons per 10 seconds in this experiment. (C) Schematic representation of a mitochondria and the effect of oligomycin on the proton fluxes generated at the F_0/F_1 synthase.

CN^- respectively induced a progressive mitochondrial depolarisation (Fig. 9A, *n*=5). However this depolarisation was not complete, as application of FCCP was still able to release more Rhod123 from the mitochondria (seen as a further increase in Rhod123 fluorescence, Fig. 9A). Moreover, the complex I inhibitor rotenone but not the complex II inhibitor malonate induced the $[Ca^{2+}]$ increase (rotenone, *n*=30; malonate, *n*=10, Fig. 9A) even though both inhibitors promote partial mitochondrial depolarisation.

Therefore, even when the mitochondrial electron transport chain is inhibited, mitochondria of mature eggs can still

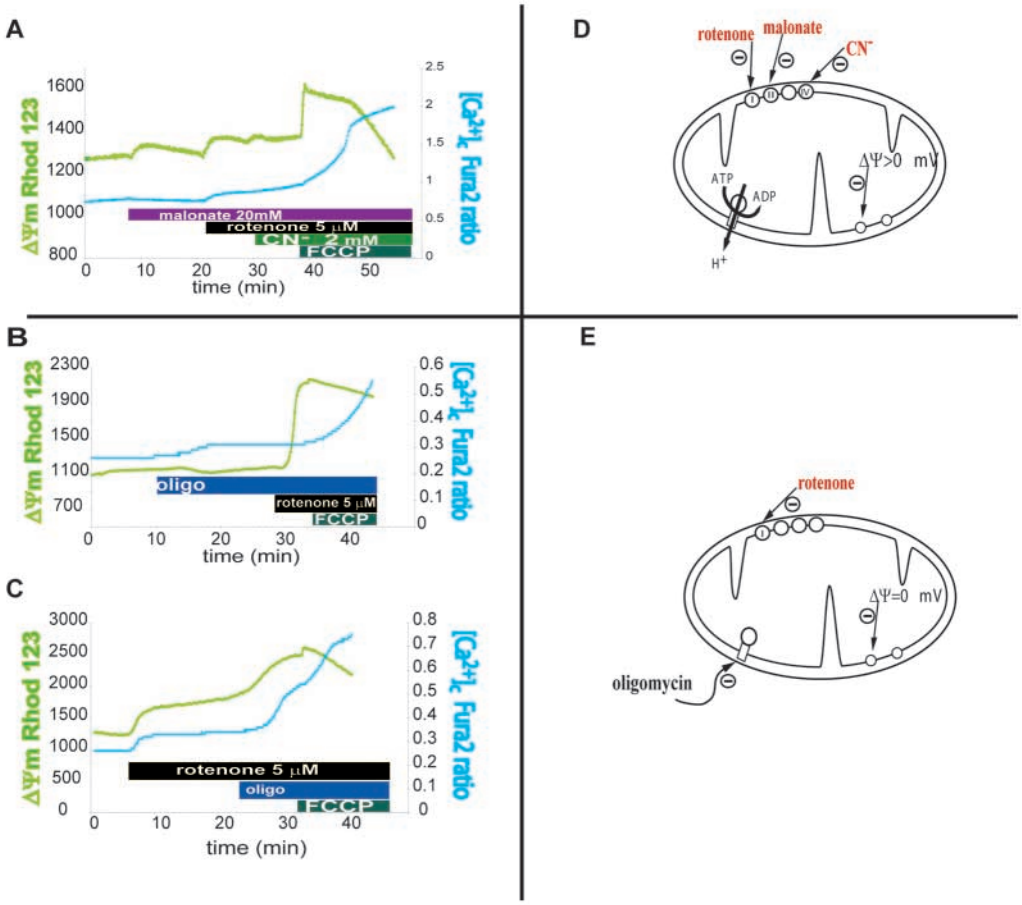

Fig. 9. Mitochondrial potential can be maintained by the reversal of the ATP synthase. (A-C) Simultaneous measurement of $[Ca^{2+}]_c$ (using fura 2 AM) and of ΔΨm (using Rhod123) in mature eggs. Where indicated, oligomycin (60 μM), FCCP (1 μM), malonate (20 mM) and rotenone (5 μM) are added to the bath. (D,E) Schematic representations of a mitochondria and the effect of mitochondrial inhibitors on the proton fluxes generated at the respiratory chain (D, CN^-, rotenone, malonate) or at the F_0/F_1 synthase (E, oligomycin).

maintain a potential. Maintenance of a mitochondrial potential during inhibition of the electron transport chain is probably caused by the reversal of the ATP synthase, which acts as a proton translocating ATPase, hydrolysing ATP and pumping protons from the mitochondrial matrix (Fig. 9D). Accordingly, when the ATP synthase was blocked by oligomycin prior to the perfusion of the complex I inhibitor rotenone, rotenone on its own completely collapsed the mitochondrial potential (Fig. 9B). A further indication that the ATP synthase was acting in reverse mode is shown in Fig. 9C (n=4). In this experiment oligomycin, perfused after rotenone, provoked a depolarisation of the mitochondria as opposed to the hyperpolarisation induced by oligomycin alone (Fig. 9B). In this case, inhibition of the reversed ATP synthase stopped the outward proton flux that was maintaining the potential.

Our protocol revealed that there was no measurable delay between the mitochondrial depolarisation (or hyperpolarisation for oligomycin perfusion) and the $[Ca^{2+}]$ increase. The collapse of mitochondrial potential or inhibition of ATP synthase was in all cases matched with an increase in intracellular $[Ca^{2+}]$, suggesting a strong link between ATP demand and Ca^{2+} homeostasis.

Together these observations reveal that the mitochondrial potential is tightly regulated in the mouse egg and that the ATP synthase is a major regulator of the mitochondrial potential.

Close apposition of ER and mitochondria in the mouse egg

The observations of Ca^{2+} driven oscillations in mitochondrial activity as well as the finding of a strong link between ATP demand and Ca^{2+} homeostasis both suggest that functional interactions exist between intracellular ER stores and the mitochondria. We therefore imaged ER and mitochondria simultaneously in a mouse egg to assess their relative distribution. Simultaneous imaging of ER and mitochondria in a mature MII egg revealed a close apposition of mitochondria and ER (Fig. 10). Strikingly, at high magnification it can be seen that an aggregation of mitochondria is embedded in sheets of ER (Fig. 10B,C). Such spatial organisation of ER and mitochondria provides a structural support for the functional interactions between ER and mitochondria that we have shown to participate in the maintenance of a low resting $[Ca^{2+}]_c$.

Discussion

In this study, we have investigated mitochondrial activity in the mouse egg in order to determine the source of energy in the egg and its relationships with the sperm triggered Ca^{2+} transients. We found that mitochondria are active in the mouse egg and early embryo and have established that sperm-triggered $[Ca^{2+}]$ oscillations are able to pace mitochondrial metabolism. Using mitochondrial inhibitors we further demonstrate the vital role mitochondrial metabolism plays in

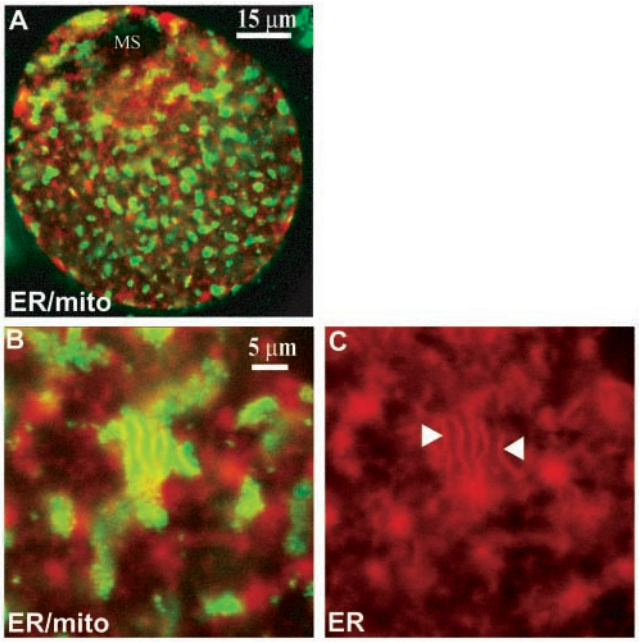

Fig. 10. Confocal imaging reveals close apposition of mitochondria and ER in a mature egg. (A) General view of a mature egg stained for mitochondria (green) and ER (red) showing mitochondrial aggregates and an ER network dispersed in the whole cytoplasm except in the region of the meiotic spindle (MS) marking the animal pole of the egg. (B,C) Higher magnification view of a mitochondrial aggregate and its relationship with the ER network. It can be clearly seen that strands of ER are intermingled in the aggregate of mitochondria (two of them are indicated by white arrowheads).

the maintenance of a low $[Ca^{2+}]_c$ at rest and in sustaining the sperm-triggered $[Ca^{2+}]$ oscillations that are necessary for triggering early development. Our observations provide insights into how ATP supply is stimulated at fertilisation to meet for the increased energy demand associated with the activation of development and into how energy production regulates Ca^{2+} homeostasis in the mammalian early embryo.

Mitochondria are metabolically active in mouse eggs

A number of observations show that mitochondria are active in mouse eggs. First, blocking selectively the mitochondrial F0/F1 ATP synthase with oligomycin causes the rapid depletion of intracellular ATP levels, demonstrating that a steady level of ATP is maintained in the unfertilised egg by mitochondrial oxidative phosphorylation. This supports the idea that ATP is primarily supplied by oxidation of mitochondrial substrates (such as pyruvate), which is consistent with the known requirement for pyruvate during early development (Leese, 1995). The data appear to be inconsistent with the suggestion that mitochondria are immature and inactive in the early embryo (Trimarchi et al., 2000). Despite a low respiratory rate (Houghton et al., 1996; Trimarchi et al., 2000), we show that mitochondria are active and phosphorylating in the mouse egg and the large number of mitochondria in mammalian eggs (around 100,000) (Piko and Taylor, 1987; Barritt et al., 2002) make a crucial contribution to ATP supply. Most remarkably, and in strong contrast to most cells studied, the rapid decrease in cellular ATP to levels crucial for the regulation of $[Ca^{2+}]$ in response to oligomycin suggests that the resting MII oocyte has a high turnover of ATP and that mitochondrial ATP generation and local ATP consumption must be delicately balanced.

We also observed that the F_0/F_1 synthase is a major regulator of the mitochondrial potential as respiratory chain inhibitors can completely depolarise the mitochondria only if the F_0/F_1 synthase is blocked. As a result, a decrease in mitochondrial potential can be offset by reversal of the F_0/F_1 synthase with a resulting extrusion of H^+ from the mitochondrial matrix that restores the mitochondrial potential. This tight regulation of mitochondrial potential may explain why we failed to observe any changes in mitochondrial potential during the sperm-triggered $[Ca^{2+}]$ oscillations (not shown) even though mitochondrial respiratory activity is upregulated by these Ca^{2+} transients (see next section). The mitochondrial potential must be maintained to support ATP synthesis; however, a high mitochondrial potential will favour production of deleterious reactive oxygen species (ROS) (Merry, 2002). As mouse eggs and embryos are sensitive to oxidative stress (Liu et al., 2000), the mitochondrial potential may be maintained to a value that allows an efficient phosphorylation of ADP while minimising ROS production.

Ca^{2+} transients at fertilisation stimulate mitochondrial activity

By imaging the mitochondrial autofluorescence, we demonstrate Ca^{2+} driven oscillations in mitochondrial activity, each Ca^{2+} transient entraining the transient reduction of NAD^+ and flavoproteins. Our observations are best explained by the following scheme: Ca^{2+} released into the cytosol enters the mitochondrial matrix to activate the Krebs cycle (Fig. 11). Activation of the Krebs cycle would provide more NADH and lead to the reduction of flavoproteins. The increased provision of reducing equivalents (NADH and $FADH_2$) will stimulate mitochondrial respiration and increase ATP generation, causing a progressive re-oxidation by the electron transport chain until a subsequent Ca^{2+} transient stimulates further reduction and restarts the cycle. This role of Ca^{2+} in the mitochondrial matrix allows the close matching of ATP production to energy demand: after triggering ATP-consuming reactions in the cytosol, Ca^{2+} upregulates the synthesis of ATP in the mitochondria (Fig. 11). Indeed, after fertilisation, approximately 3 μM of free Ca^{2+} is released into the cytosol and must then be cleared from the cytosol by active transport by the SERCAs and by the PMCAs. This released Ca^{2+} also stimulates ATP-dependent exocytosis of cortical granules and the extrusion of the second polar body, which also requires ATP. Therefore synthesis of ATP is required to maintain the ATP level after fertilisation. Matching ATP supply and demand via Ca^{2+} regulation of the Kreb's cycle provides a mechanism of maintaining low oxidative phosphorylation that, in turn, minimises the production of potentially damaging ROS by the electron transport chain (Harvey et al., 2002; Merry, 2002).

Role of mitochondria in Ca^{2+} homeostasis and sperm-triggered $[Ca^{2+}]$ oscillations

Contrasting with the study of Liu et al. (Liu et al., 2001), the Ca^{2+} probe Rhod2 AM used in somatic cells to monitor mitochondrial Ca^{2+} concentration, $[Ca^{2+}]_{mito}$ (Duchen, 2000; Duchen et al., 2003), in our hands, did not partition into

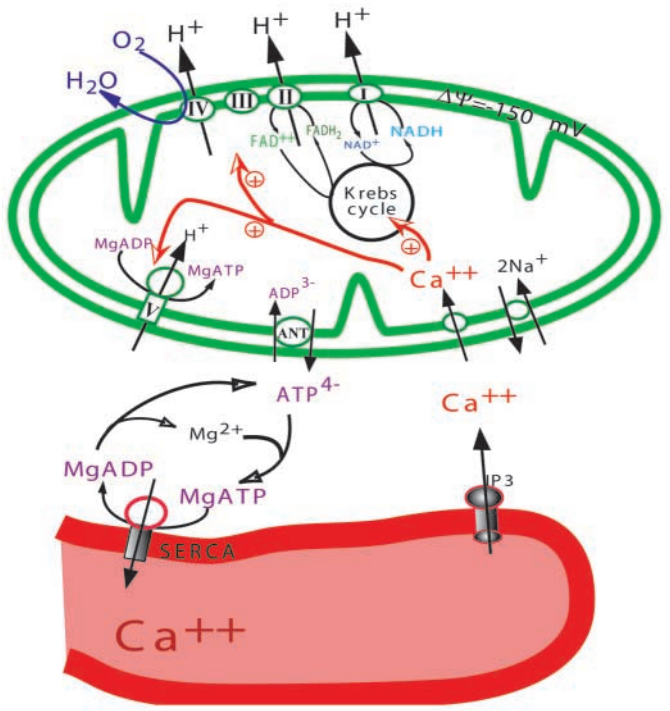

Fig. 11. A model depicting the functional interactions between ER and mitochondria in the mouse egg. After Ca^{2+} is released from the ER into the cytosol via Ins(1,4,5)P_3 receptors it can be taken up by the mitochondria. In the mitochondrial matrix, Ca^{2+} will stimulate the Kreb's cycle as well as the electron transport chain and the F_0/F_1 synthase that phosphorylates ADP. ATP is then transported out of the mitochondria via the activity of the adenine nucleotide translocase (ANT) and the cytosolic ATP will be consumed by the SERCA pumps to restore the resting $[Ca^{2+}]_c$ and refill the ER.

mitochondria of the mouse egg (Fig. 3); therefore the changes in $[Ca^{2+}]_{mito}$ could not be measured directly. Nevertheless, we investigated the role mitochondria play in Ca^{2+} homeostasis and in sperm-triggered $[Ca^{2+}]$ oscillations by applying different mitochondrial inhibitors onto mouse eggs. We found that the mitochondrial uncoupler FCCP and the complex I (rotenone) and complex IV (CN^-) inhibitors but not the complex II inhibitor (malonate) induce a Ca^{2+} leak from the intracellular ER stores. The appearance of this Ca^{2+} leak is due to ATP depletion, as oligomycin alone also provokes this leak. Therefore, in the mature egg, mitochondrial ATP production provides the energy used by the SERCA pumps to maintain a low resting $[Ca^{2+}]_c$ (Fig. 11). The innocuity of the complex II inhibitor malonate suggests that mitochondria mostly oxidise complex I-linked substrates (i.e. pyruvate) for oxidative phosphorylation, consistent with the known preferred energetic substrate of the mouse egg (Leese, 1995; Leese, 2002).

The first rise in Ca^{2+} induced by mitochondrial inhibitors is followed by a larger secondary increase. The source of Ca^{2+} of the latter increase, presumably arising after a more pronounced ATP depletion, lies in the extracellular medium. Thus, ATP depletion in the egg affects first the SERCAs then the PMCAs. The rapid inhibition of the SERCAs by ATP depletion suggests that the activity of the SERCAs strictly depends on mitochondrial ATP production. The delay between the apparent failure of the SERCAs and the PMCAs is best explained if inhibition of mitochondrial ATP synthesis affects first local ATP supply close to the sites of demand by SERCA, and while the global [ATP] only falls sufficiently to cause failure of the PMCA later. These observations strongly suggest a functional coupling between ER and mitochondria mediated by ATP (Fig. 11). Simultaneous imaging of ER and mitochondria revealed a close apposition of mitochondria organised in aggregates around sheets of ER that is consistent with a functional interplay between these organelles. It will be interesting to determine whether SERCA pumps are especially enriched in the sheets of ER surrounded by mitochondria.

The crucial role for mitochondria in sustaining sperm-triggered $[Ca^{2+}]$ oscillations is to provide ATP whereas buffering of cytosolic Ca^{2+} by mitochondria seems to have no major influence on the pattern of the $[Ca^{2+}]$ oscillations. First, $[Ca^{2+}]$ oscillations can continue for several minutes after FCCP-induced mitochondrial depolarisation (which prevents mitochondria from sequestering cytosolic Ca^{2+}). Second, oligomycin perfusion that does not hamper Ca^{2+} sequestering by mitochondria is still able to inhibit the $[Ca^{2+}]$ oscillations. The importance of mitochondrial ATP production was further illustrated by fertilisation in a medium devoid of any energetical substrates. In such cases, $[Ca^{2+}]$ oscillations were disrupted. The return of pyruvate to the medium was able to provoke the resumption of the $[Ca^{2+}]$ oscillations. Together, these observations characterise a crucial role for mitochondrial oxidative phosphorylation at the activation of development.

Conclusion

The tight coupling of ATP supply and demand proposed in this study provides a major advantage for early mammalian development. The maternal inheritance of mitochondria requires that mitochondria are protected from potentially damaging ROS. The maintenance of a low level of oxidative phosphorylation that can be stimulated on an increase in ATP demand provides one means of lowering exposure of mitochondria to damaging oxidative stress. Our data suggest that Ca^{2+} is the functional link that provides a mechanism for coupling ATP supply and demand. As maternal aging is associated with increased oxidative stress in human eggs (Tarin, 1996) it will interesting to define whether mitochondrial physiology and the coupling of ATP supply and demand are impaired in eggs from aged women.

We thank Israa Mazin Al-Shakarchi for preliminary results on the mitochondrial inhibitors, and Andrey Abramov for insightful discussions during the course of this work. This work was supported by grants from the MRC, the Wellcome Trust and EC. R.D. is supported by a Marie Curie Individual Fellowship of the EC.

References

Allue, I., Gandelman, O., Dementieva, E. and Ugarova, N. (1996). Evidence for rapid consumption of millimolar concentrations of cytoplasmic ATP during rigor-contracture of metabolically compromised single cardiomyocytes. *Biochem. J.* **319**, 463-469.

Barbehenn, E. K., Wales, R. G. and Lowry, O. H. (1974). The explanation for the blockade of glycolysis in early mouse embryos. *Proc. Natl. Acad. Sci. USA* **71**, 1056-1060.

Barritt, J. A., Kokot, M., Cohen, J., Steuerwald, N. and Brenner, C. A. (2002). Quantification of human ooplasmic mitochondria. *Reprod. Biomed. Online* **4**, 243-247.

Biggers, J. D., McGinnis, L. K. and Raffin, M. (2000). Amino acids and

preimplantation development of the mouse in protein-free potassium simplex optimized medium. *Biol. Reprod.* **63**, 281-293.

Brini, M., Coletto, L., Pierobon, N., Kraev, N., Guerini, D. and Carafoli, E. (2003). A comparative functional analysis of plasma membrane Ca2+ pump isoforms in intact cells. *J. Biol. Chem.* **278**, 24500-2458.

Carroll, J. (2000). Na+-Ca2+ exchange in mouse oocytes: modifications in the regulation of intracellular free Ca2+ during oocyte maturation. *J. Reprod. Fertil.* **118**, 337-342.

Carroll, J. (2001). The initiation and regulation of Ca2+ signalling at fertilisation in mammals. *Semin. Cell Dev. Biol.* **12**, 37-43.

Duchen, M. R. (1992). Ca(2+)-dependent changes in the mitochondrial energetics in single dissociated mouse sensory neurons. *Biochem. J.* **283**, 41-50.

Duchen, M. (2000). Mitochondria and calcium: from cell signalling to cell death. *J. Physiol.* **529**, 57-68.

Duchen, M. R. and Biscoe, T. J. (1992). Relative mitochondrial membrane potential and [Ca2+]i in type I cells isolated from the rabbit carotid body. *J. Physiol.* **450**, 33-61.

Duchen, M. R., Surin, A. and Jacobson, J. (2003). Imaging mitochondrial function in intact cells. *Methods Enzymol.* **361**, 353-389.

Ducibella, T., Huneau, D., Angelichio, E., Xu, Z., Schultz, R. M., Kopf, G. S., Fissore, R., Madoux, S. and Ozil, J. P. (2002). Egg-to-embryo transition is driven by differential responses to Ca^{2+} oscillation number. *Dev. Biol.* **250**, 280-291.

Dumollard, R., Carroll, J., Dupont, G. and Sardet, C. (2002). Calcium wave pacemakers in eggs. *J. Cell Sci.* **115**, 3557-3564.

Dumollard, R., Hammar, K., Porterfield, M., Smith, P. J., Cibert, C., Rouviere, C. and Sardet, C. (2003). Mitochondrial respiration and Ca^{2+} waves are linked during fertilisation and meiosis completion. *Development* **130**, 683-692.

Eisen, A. and Reynolds, G. T. (1985). Source and sinks for the calcium released during fertilisation of single sea urchin eggs. *J. Cell Biol.* **100**, 1522-1527.

FitzHarris, G., Marangos, P. and Carroll, J. (2003). Cell cycle-dependent regulation of structure of endoplasmic reticulum and inositol 1,4,5-trisphosphate-induced Ca2+ release in mouse oocytes and embryos. *Mol. Biol. Cell* **14**, 288-301.

Gardner, D. K., Clarke, R. N., Lechene, C. P. and Biggers, J. D. (1989). Development of a noninvasive ultramicrofluorometric method for measuring net uptake of glutamine by single preimplantation mouse embryos. *Gamete Res.* **24**, 427-438.

Hajnoczky, G., Robb-Gaspers, L., Seitz, M. B. and Thomas, A. (1995). Decoding of cytosolic calcium oscillations in the mitochondria. *Cell* **82**, 415-424.

Hansford, R. (1994). Physiological role of mitochondrial Ca^{2+} transport. *J. Bioenerg. Biomemb.* **26**, 495-508.

Harvey, A. J., Kind, K. L. and Thompson, J. G. (2002). REDOX regulation of early embryo development. *Reproduction* **123**, 479-486.

Houghton, F. D., Thompson, J. G., Kennedy, C. J. and Leese, H. J. (1996). Oxygen consumption and energy metabolism of the early mouse embryo. *Mol. Reprod. Dev.* **44**, 476-485.

Jones, K. (1998). Ca^{2+} oscillations in the activation of the egg and development of the embryo in mammals. *Int. J. Dev. Biol.* **42**, 1-10.

Jouaville, L. S., Pinton, P., Bastianutto, C., Rutter, G. A. and Rizzuto, R. (1999). Regulation of mitochondrial ATP synthesis by calcium: evidence for a long-term metabolic priming. *Proc. Natl. Acad. Sci. USA* **96**, 13807-13812.

Kline, D. and Kline, J. T. (1992). Repetitive calcium transients and the role of calcium in exocytosis and cell cycle activation in the mouse egg. *Dev. Biol.* **149**, 80-89.

Lane, M. and Gardner, D. K. (2000). Lactate regulates pyruvate uptake and metabolism in the preimplantation mouse embryo. *Biol. Reprod.* **62**, 16-22.

Lawrence, Y., Ozil, J. P. and Swann, K. (1998). The effects of a Ca2+ chelator and heavy-metal-ion chelators upon Ca2+ oscillations and activation at fertilization in mouse eggs suggest a role for repetitive Ca2+ increases. *Biochem. J.* **335**, 335-342.

Leese, H. J. (1995). Metabolic control during preimplantation mammalian development. *Hum. Reprod. Update* **1**, 63-72.

Leese, H. J. (2002). Quiet please, do not disturb: a hypothesis of embryo metabolism and viability. *BioEssays* **24**, 845-849.

Liu, L., Trimarchi, J. R. and Keefe, D. L. (2000). Involvement of mitochondria in oxidative stress-induced cell death in mouse zygotes. *Biol. Reprod.* **62**, 1745-1753.

Liu, L., Hammar, K., Smith, P. J., Inoue, S. and Keefe, D. L. (2001). Mitochondrial modulation of calcium signaling at the initiation of development. *Cell Calcium* **30**, 423-433.

Mak, D., McBride, S. and Foskett, J. (1999). ATP regulation of type 1 inositol 1,4,5-trisphosphate receptor channel gating by allosteric tuning of Ca^{2+} activation. *J. Biol. Chem.* **274**, 22231-22237.

Mak, D., McBride, S. and Foskett, J. (2001). ATP regulation of recombinant type 3 inositol 1,4,5-trisphosphate receptor gating. *J. Gen. Physiol.* **117**, 447-456.

Marangos, P., FitzHarris, G. and Carroll, J. (2003). Ca2+ oscillations at fertilisation in mammals are regulated by the formation of pronuclei. *Development* **130**, 1461-1472.

Masters, B. and Chance, B. (1993). Redox confocal imaging: intrinsic fluorescent probes of cellular metabolism. In *Fluorescent and Luminescent Probes for Biological Activity* (ed. W. Mason), pp. 44-56. London: DB Sattelle.

McCormack, J. G. and Denton, R. M. (1993). The role of intramitochondrial Ca2+ in the regulation of oxidative phosphorylation in mammalian tissues. *Biochem. Soc. Trans.* **21**, 793-799.

Merry, B. J. (2002). Molecular mechanisms linking calorie restriction and longevity. *Int. J. Biochem. Cell Biol.* **34**, 1340-1354.

Motta, P. M., Nottola, S. A., Makabe, S. and Heyn, R. (2000). Mitochondrial morphology in human fetal and adult female germ cells. *Hum. Reprod.* **15 Suppl. 2**, 129-147.

Ozil, J. and Huneau, D. (2001). Activation of rabbit oocytes: the impact of the Ca^{2+} signal regime on development. *Development* **128**, 917-928.

Pepperell, J. R., Kommineni, K., Buradagunta, S., Smith, P. J. and Keefe, D. L. (1999). Transmembrane regulation of intracellular calcium by a plasma membrane sodium/calcium exchanger in mouse ova. *Biol. Reprod.* **60**, 1137-1143.

Piko, L. and Taylor, K. D. (1987). Amounts of mitochondrial DNA and abundance of some mitochondrial gene transcripts in early mouse embryos. *Dev. Biol.* **123**, 364-374.

Pralong, W. F., Spat, A. and Wollheim, C. B. (1994). Dynamic pacing of cell metabolism by intracellular calcium transients. *J. Biol. Chem.* **269**, 27310-27314.

Rizzuto, R., Bernardi, P. and Pozzan, T. (2000). Mitochondria as all-round players of the calcium game. *J. Physiol.* **529**, 37-47.

Sathananthan, A. H. and Trounson, A. O. (2000). Mitochondrial morphology during preimplantational human embryogenesis. *Hum. Reprod.* **15 Suppl. 2**, 148-159.

Stricker, S. A. (1999). Comparative biology of calcium signaling during fertilisation and egg activation in animals. *Dev. Biol.* **211**, 157-176.

Sturmey, R. G. and Leese, H. J. (2003). Energy metabolism in pig oocytes and early embryos. *Reproduction* **126**, 197-204.

Swann, K. and Ozil, J. P. (1994). Dynamics of the calcium signal that triggers mammalian egg activation. *Int. Rev. Cytol.* **152**, 183-222.

Tarin, J. J. (1996). Potential effects of age-associated oxidative stress on mammalian oocytes/embryos. *Mol. Hum. Reprod.* **2**, 717-724.

Territo, P., Mootha, V., French, S. and Balaban, R. (2000). Calcium activation of heart mitochondrial oxidative phosphorylation: role of the F0/F1-ATPase. *Am. J. Physiol.* **278**, C423-C435.

Trimarchi, J., Liu, L., Porterfield, D., Smith, P. and Keefe, D. (2000). Oxidative phosphorylation-dependent and-independent oxygen consumption by individual preimplantation mouse embryos. *Biol. Reprod.* **62**, 1866-1874.

Van Blerkom, J., Davis, P., Mathwig, V. and Alexander, S. (2002). Domains of high-polarized and low-polarized mitochondria may occur in mouse and human oocytes and early embryos. *Hum Reprod.* **17**, 393-406.

Wilding, M., de Placido, G., de Matteo, L., Marino, M., Alviggi, C. and Dale, B. (2003). Chaotic mosaicism in human preimplantation embryos is correlated with a low mitochondrial membrane potential. *Fertil. Steril.* **79**, 340-346.